

404 **Appendix**

405 **Computing environment**

406 MNIST benchmark runs were executed on a stand-alone x86 PC using 8 CPU cores, 8 GB RAM,
407 and no GPUs, The system installs Windows 10, Jupyter notebook 6.4.3, python 3.8.5, and PyTorch
408 1.9.1. We used MNIST data in PyTorch divided by a batch size of 128.

409 CIFAR10&100 benchmark runs were executed on an x86 cluster using 8 cores in a single node,
410 typically 4-5 GB RAM allocated, and no GPUs, The system installs Linux version 8.5. python
411 3.6.9, and PyTorch 1.2.0. We used CIFAR10&100 data in PyTorch divided by a batch size of 256².

412 **Present limitations**

413 Currently, the neural network representation is not perfectly asynchronous because of Eq. 32 to
414 pipeline the coarse-grained dynamics. However, this limitation may make sense considering that
415 biological brains also use slow brain waves to lively regulate their operations. The strategy can
416 reduce w_{ij} update frequency without much affecting online tracking performance.

417 Another limitation is that synaptic networks consisting of the axon, synapse, and dendrite are as-
418 sumed linear, and nonlinear operations are presently dumped into neurons in conjunction with σ_1
419 and σ_2 . For example, batch normalization is a nonlinear operation that may be implemented by
420 more naturally adjusting the amplitude and delay distributions of neural signals. Computing the loss
421 function (in this research, the cross-entropy loss was used) is another case in which the computation
422 is now performed outside operator-discretized networks. Instead of making the synaptic network
423 nonlinear in a Cartesian-product state space, it may stay linear in a tensor product state space, which
424 is not entirely impossible as stated later.

425 Furthermore, this representation expects the data to take an event-driven (e.g., time-stamped) format,
426 rather than synchronous streams like video data. In latter cases, some sort of front-end to convert
427 frame-synchronous data may help.

428 **Related topics in AI**

429 If the input data streams are appropriately arranged, the application of the idea to a variety of tempo-
430 ral ANNs beyond tSNNs should be of interest as a follow-on investigation. The operator-discretized
431 representation will make sense for encoding information into temporal sequences and processing
432 them in time as seen in spike trains in biological neural systems. The fine-grained spike dynamics
433 can be nicely decoupled from the coarse-grained behavioral one. We may regard what is happen-
434 ing in the fine-grained part as a sort of vector to time conversion, which is somewhat opposite to
435 time2vec [A1]. This approach will work better when the fine-grained dynamics is dominated by
436 predefined temporal correlations, rather than blindly learned from data.

437 The operator representation may be combined with other well-established machine learning tech-
438 niques, such as kernel methods [A2], as a means to constitute appropriate basis sets in large spa-
439 tiotemporal dimensions. The nonstationary operators can add unique value to such methods by con-
440 sistently handling temporal dynamics using amplitude and/or temporal coding. Adjoint operators
441 will naturally incorporate backward dynamics for learning. The use of log probability is popular,
442 such as in log-likelihood or Viterbi algorithm, to better deal with product events. Relating the log
443 of the probability to the Euclidean norm of the signal amplitude as in Eq. 9 for $p = 2$ is consistent
444 with, for example, what has been done in Viterbi algorithm under Gaussian noise [A3].

445 Our emulation strategy can become a searchlight to explore future neuromorphic HW. The bidirec-
446 tional and elastic nature of our operators may help to natively investigate other physically-oriented
447 (e.g., mechanical) models, such as equilibrium propagation [A4]. The faster turnaround of the pro-
448 posed emulation methodology will facilitate detailed comparison across multiple design choices,
449 for example, digital and analog spiking [A5, A6] against reduced precision approaches [A7] using
450 modern AI workloads. We believe that temporal coding is essential for neuromorphic HW to be
451 truly as efficient as the biological brain. Encoding information into the pulse width may rather be
452 considered as non-return-zero rSNNs without much information temporarily.

²Similar results with imagenet in multinode distributed data-parallel to be published upon approval

453 **Biological implications**

454 Though the present research is on artificial neural networks, originally initiated by treating neural
 455 signals as slowly-traveling elastic waves [31, 32], there are growing pieces of works on the impor-
 456 tance of wave dynamics in biological neural networks as well [33, 34]. Thus, it may also be worth
 457 investigating more biological neuron models, such as Izhikevich neurons [A8] within our represen-
 458 tation. Specific functional forms for σ_1 and σ_2 will affect amplifying and/or damping of collective
 459 wave dynamics, which may better elucidate what is happening in biological systems.

460 Since the geometrical size of spike signals is less than typical axon-synapse-dendrite network sizes,
 461 it makes sense, also from a biological standpoint, to explicitly deal with the traveling wave dynamics
 462 of spike signals. The width in size of a spike signal is ~ 1 mm for a velocity ~ 1 m/s and a width in
 463 time of ~ 1 ms. Thus, the axon-synapse-dendrite networks need to be treated as distributed entities,
 464 rather than lumped. The biological implications of present LC TL models for axons and dendrites
 465 should be argued further in comparison to the conventional RC cable models. LC TLs are superior
 466 in better transmitting signal energy and information without dissipation. However, since the origin
 467 of a reasonable amount of L is still controversial, the use of L in the biology literature is limited [A9]
 468 to our knowledge.

469 Here, we speculate that significant L could be caused by more than 4 orders of magnitude heavier
 470 masses of ions than that of electrons (3.81754×10^{-23} g for Na^+ and $9.1093837 \times 10^{-28}$ g for e^-).
 471 This is because the kinetic inductance L_K due to the elastic inertia without scattering given by the
 472 following equation [A10] is also more than 4 orders of magnitude higher:

$$L = L_{EM} + L_K, \quad L_K = \frac{m}{nq^2} \frac{l}{A} \quad (\text{A1})$$

473 where m is mass, n density, q charge, l length, A area. For the electric TLs, it is well known that,
 474 though microscopic electron motions are diffusive, the coherent electrical signal waves driven by the
 475 macroscopic charge density offset is not much affected by them. It should be carefully investigated
 476 further whether the same situation holds in more electro-mechanical biological environments with
 477 much more complex ion dynamics, and therefore, whether the heavier ion masses can indeed make
 478 L_K a dominant component as Eq. A1 indicates.

479 Ingress and egress operators can naturally represent orthodromic and antidromic spike transmis-
 480 sions [A11]. Thus, our operator formalism may help to systematically model bidirectional spike
 481 transmissions in biological systems.

482 **Perspective on future AI and QC**

483 It is one of the primary agendas in future computing how AI and QC would evolve in parallel
 484 with conventional computing systems. The present approach will shed new light on it as "AI \cup
 485 QC" arguments, alternative to historical "AI \cap QC" [A12], and facilitate us to unlock unknown
 486 mechanisms of the brain. This is because the present idea seems to suggest that classical wave
 487 dynamics alone can achieve some limited functionalities of QC by taking advantage of Euclidean-
 488 norm computing features that have been considered unique to QC [29].

489 Figure A1 (a) illustrates delay and sum beamforming with delay precoding. It exemplifies how the
 490 Euclidean norm can enhance the contrast between desired and undesired signals for better perfor-
 491 mance under a given energy budget (known as the beamforming gain in wireless literature [30]).
 492 Freespace should be replaced with a waveguide network for neural signals and the geometrical size
 493 will be orders of magnitude reduced as the signal velocity is reduced from the speed of light (3.0
 494 $\times 10^8$ m/s) to ~ 1 m/s [31, 32]. Well-arranged attenuated superpositions of neural signals from pre-
 495 ceding neurons can increase desired signal amplitudes with constructive interference, and decrease
 496 undesired ones with destructive interference. We still need to carefully work on how to exploit this
 497 feature in future computing, but let us discuss some interesting possibilities below.

498 Grover algorithm is well known as a QC algorithm with quadratic speed-up by using amplitude
 499 amplification. Here, we would like to argue that the same algorithm is also possible with cubits as
 500 shown in Fig.A1(b). By using n normalized full cubits instead of $m = \log_2 n$ qubits, the state $||\rho\rangle\rangle$
 501 is given as

$$||\rho\rangle\rangle = ||\rho_1\rangle\rangle \oplus \dots \oplus ||\rho_n\rangle\rangle = ||\rho'\rangle\rangle \oplus ||\rho''\rangle\rangle. \quad (\text{A2})$$

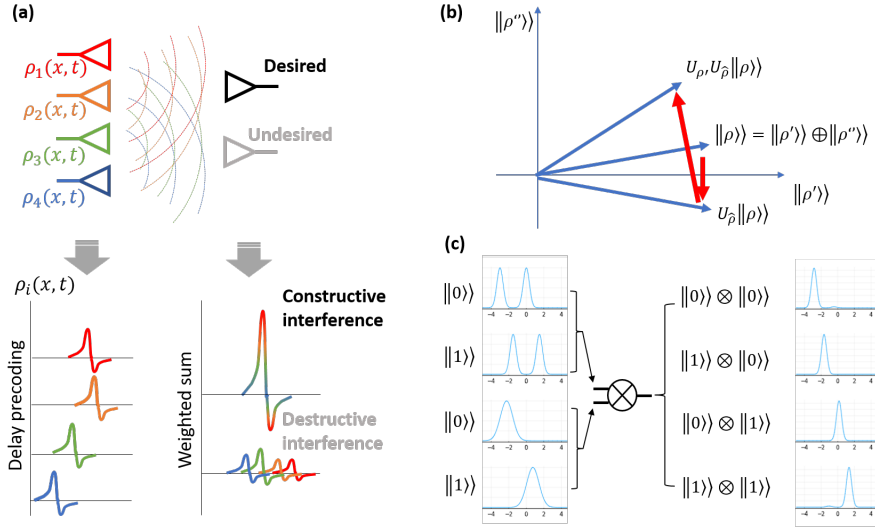


Figure A1: (a) Delay and sum beamforming in wireless communications (freespace is to be replaced with a waveguide network for neural signals); (b) Grover algorithm with cubits; (c) A tensor product state with two cubits. All take advantage of classical wave physics with the Euclidean norm.

502 This corresponds to the following m qubit state:

$$|\rho\rangle = \rho_1 |0_0\rangle \otimes |0_1\rangle \otimes \dots \otimes |0_m\rangle \oplus \rho_2 |1_0\rangle \otimes |0_1\rangle \otimes \dots \otimes |0_m\rangle \oplus \dots \rho_n |1_0\rangle \otimes |1_1\rangle \otimes \dots \otimes |1_m\rangle. \quad (\text{A3})$$

503 So, n cubits and m qubits span the same state space of $n = 2^m$ dimension. Then the following
 504 exactly the same two unitary operations, starting with $|\rho\rangle = |\rho^{init}\rangle$, are repeated $O(n^{1/2})$ times
 505 on the cubit state:

$$U_{\rho'} = 2|\rho\rangle\langle\rho| - I, \quad (\text{A4})$$

506 and

$$U_{\rho''} = \begin{cases} -|\rho_i\rangle\langle\rho_i| & \text{if } |\rho_i\rangle = |\rho''\rangle, \\ |\rho_i\rangle\langle\rho_i| & \text{otherwise.} \end{cases} \quad (\text{A5})$$

507 Though an exponentially larger number of cubits is required (this may make sense considering
 508 $\sim 10^{11}$ neurons in our brain), the complications associated with encoding n data into m qubits can
 509 be avoided.

510 In contrast, the exponential speedup in specific QC algorithms, such as quantum Fourier transform
 511 and factoring, seems difficult since they take full advantage of tensor product state spaces. Though
 512 tensor product state of cubits, such as

$$|\rho_i\rangle \otimes |\rho_j\rangle \quad (\text{A6})$$

513 can be defined and constructed with signal multipliers as exemplified in Fig. A1(c), the states can
 514 entangle only locally and the dimension is limited by the bandwidth.

515 There are other distinct differences to be mentioned. The interference discussed here of classical
 516 waves can occur for signals from different sources. This is a noticeable difference since the qubits
 517 interfere only from the same sources. In addition, the coherence time of classical waves can be quite
 518 long even at room temperature, as is observed in sound waves, radio waves, ocean waves, and so
 519 on [31–34].

520 **References**

- 521 [A1] Kazemi, S. M., Goel, R., Eghbali, S., Ramanan, J., Sahota, J., Thakur, S., Wu, W.,
522 Smyth, C., Poupart, P. & Brubaker, M. Time2Vec: Learning a Vector Representation of Time
523 *arXiv:1907.05321v1* (2019).
- 524 [A2] Bishop, C. M. *Pattern Recognition and Machine Learning* (Springer, 2006).
- 525 [A3] Forney, G. D. The Viterbi Algorithm *Proc. IEEE* **61**, 268–278 (1973).
- 526 [A4] Scellier, B. & Bengio, Y. Equilibrium Propagation: Bridging the Gap between Energy-Based
527 Models and Backpropagation. *Front. Comput. Neurosci.* **11**, 24 (2017).
- 528 [A5] Merolla, P. A., Arthur, J. V., Alvarez-Icaza, R., Cassidy, A. S., Sawada, J., Akopyan, F., Jack-
529 son, B. L., Imam, N., Guo, C., Nakamura, Y., Brezzo, B., Vo, I., Esser, S. K., Appuswamy, R.,
530 Taba, B., Amir, A., Flickner, M., Risk, W. P., Manohar, R. & Modha, D. S. A million spiking-
531 neuron integrated circuit with a scalable communication network and interface. *Science* **345**,
532 668–673 (2014).
- 533 [A6] Ambrogio, S., Narayanan, P., Tsai, H., Shelby, R. M., Boybat, I., di Nolfo, C., Sidler, S.,
534 Giordano, M., Bodini, M., Farinha, N. C. P., Killeen, B., Cheng, C., Jaoudi, Y. & Burr, G. W.
535 Equivalent-accuracy accelerated neural-network training using analogue memory. *Nature* **558**,
536 60–67 (2018).
- 537 [A7] Sun, X., Wang, N., Chen, C.-y., Ni, J.-m., Agrawal, A., Cui, X., Venkataramani, S.,
538 Maghraoui, K. E., Srinivasan, V. & Gopalakrishnan, K. Ultra-Low Precision 4-bit Training of
539 Deep Neural Networks. *NeurIPS* (2020).
- 540 [A8] Gerstner, W. & Kistler, W. M. *Spiking neuron models: single neurons, populations, plasticity*
541 (Cambridge University Press, 2002).
- 542 [A9] Wang, H., Wang, J., Cai, G., Liu, Y., Qu, Y. & Wu, T. A Physical Perspective to the Induc-
543 tive Function of Myelin—A Missing Piece of Neuroscience. *Front. Neural Circuits* **14**, 562005
544 (2021).
- 545 [A10] https://en.wikipedia.org/wiki/Kinetic_inductance.
- 546 [A11] Li, S., Arbuthnott, G. W., Jutras, M. J., Goldberg, J. A. & Jaeger, D. Resonant Antidromic
547 Cortical Circuit Activation as a Consequence of High-Frequency Subthalamic Deep-Brain Stim-
548 ulation *J. Neurophysiol.* **98**, 3525—3537 (2007).
- 549 [A12] Hameroff, S. & Penrose, R. Orchestrated Objective Reduction of Quantum Coherence in
550 Brain Microtubules: The "Arch OR2" Model for Consciousness *Toward a Science of Conscious-
551 ness - The First Tucson Discussions and Debates* 507—540 (1996).